

## Concentration-dependent photoluminescence of Te-doped $\text{In}_{0.14}\text{Ga}_{0.86}\text{As}_{0.13}\text{Sb}_{0.87}$

This article has been downloaded from IOPscience. Please scroll down to see the full text article.

2006 J. Phys.: Condens. Matter 18 10861

(<http://iopscience.iop.org/0953-8984/18/48/013>)

View [the table of contents for this issue](#), or go to the [journal homepage](#) for more

Download details:

IP Address: 129.252.86.83

The article was downloaded on 28/05/2010 at 14:41

Please note that [terms and conditions apply](#).

# Concentration-dependent photoluminescence of Te-doped $\text{In}_{0.14}\text{Ga}_{0.86}\text{As}_{0.13}\text{Sb}_{0.87}$

J Díaz-Reyes<sup>1</sup>, J G Mendoza-Álvarez<sup>2</sup> and M L Gómez-Herrera<sup>3</sup>

<sup>1</sup> CIBA-IPN, Ex-Hacienda de San Juan Molino Km 1.5, Tepetitla, Tlaxcala 90700, Mexico

<sup>2</sup> Departamento de Física, CINVESTAV-IPN, Apartado Postal 14-740, México, DF 07000, Mexico

<sup>3</sup> CICATA-IPN, Unidad Legaria, Avenida Legaria 694, Colonia Irrigación, México, DF 11500, Mexico

E-mail: [jdiazr2001@yahoo.com](mailto:jdiazr2001@yahoo.com)

Received 11 May 2006, in final form 12 September 2006

Published 17 November 2006

Online at [stacks.iop.org/JPhysCM/18/10861](http://stacks.iop.org/JPhysCM/18/10861)

## Abstract

Quaternary layers of N-type  $\text{In}_x\text{Ga}_{1-x}\text{As}_y\text{Sb}_{1-y}$  were grown by liquid phase epitaxy on (100) GaSb substrates under lattice-matching conditions. Low-temperature photoluminescence spectra were obtained as a function of tellurium concentration. These spectra were interpreted taking into account the nonparabolicity of the conduction band. Calculations of the peak position and photoluminescence transitions were performed. Both the band filled as well as band tailing effects due to Coulomb interaction of free carriers with ionized impurities and shrinkage due to exchange interaction between free carriers were considered in order to properly account for the observed features of the photoluminescence spectra. It is shown that the band-to-band energy transition can be used to obtain the carrier concentration in N-type  $\text{In}_x\text{Ga}_{1-x}\text{As}_y\text{Sb}_{1-y}$ , in the range from  $1 \times 10^{16}$  to  $3.42 \times 10^{18} \text{ cm}^{-3}$ .

## 1. Introduction

The III–V antimonide compounds are of interest for a great number of applications, including optical communications employing fluoride-based fibres [1], laser radar exploiting atmospheric transmission windows and remote sensing. For most of these applications, operation at room temperature is very important for attaining the desired system performance at reasonable cost [2]. The quaternary  $\text{In}_x\text{Ga}_{1-x}\text{As}_y\text{Sb}_{1-y}$  alloys are among the most promising alternative materials to the HgCdTe system, for use in infrared detectors. The alloys with direct band gap adjust between 1.7 and 4.3  $\mu\text{m}$ , and can be grown lattice-matched to GaSb, InP and InAs substrates, which may provide the basis for emitters and detectors over this entire region.

Photoluminescence (PL) of InGaAsSb has been studied by a number of authors [3, 4] and the basic recombination processes are well understood. However, there are some problems to be clarified concerning the PL of heavily doped InGaAsSb. Observations by Hawrylo and

**Table 1.** Tellurium concentrations obtained by LT-PL.

Sample	[Sb <sub>2</sub> Te <sub>3</sub> ] molar fraction	BB energy (meV)	C energy (meV)	<i>n</i> (cm <sup>-3</sup> )
CE-129	—	—	—	—
CE-122	$1.163 \times 10^{-4}$	660.5	645.4	$4.78 \times 10^{17}$
CE-104	$3.695 \times 10^{-4}$	701.5	686.1	$2.38 \times 10^{18}$
CE-125	$5.269 \times 10^{-4}$	707.8	687.3	$2.71 \times 10^{18}$
CE-124	$6.090 \times 10^{-4}$	722.1	694.6	$3.42 \times 10^{18}$

Racah [5] of abnormally large band filling in highly doped material suggest the need for a re-examination of PL data for that concentration range [6]. PL is a non-destructive technique and requires no special sample preparation. Since the exciting light typically penetrates less than a micrometre and the lateral dimensions of the excited region are of the order of the minority carrier diffusion length, PL can be used in the evaluation of thin epitaxial layers as well as for concentration mapping over large-area samples. This type of measurement cannot be done by the Hall technique which gives an average concentration and works properly only for layers on semi-insulating substrates. In order to use the technique as an assessment of the material, it is necessary to relate the observed features of the PL spectra, i.e. half-width and peak position, to the otherwise determined carrier concentration.

We report in this work a study of N-type InGaAsSb layers grown by the liquid phase epitaxy (LPE) technique on (100)-oriented GaSb substrates. The effects of high Te compensation on these layers were evaluated by low-temperature PL spectroscopy.

## 2. Experimental details

LPE growth of In<sub>x</sub>Ga<sub>1-x</sub>As<sub>y</sub>Sb<sub>1-y</sub> epilayers was carried out in a three-zone isothermal furnace in hydrogen, using the horizontal sliding boat technique. The boat was made from high purity graphite. The quaternary alloy epilayers, InGaAsSb, were grown nominally lattice-matched to vicinal high resistivity (100) GaSb substrates at 530 °C. The details of the growth conditions have been published elsewhere [7]. We have used two different methods for carrying out the doping of the epilayers. In order to achieve low electron concentrations, Te was added to the growth solution in very small quantities ( $<1.63 \times 10^{-5}$  molar fraction), due to the high Te segregation coefficient. To accomplish this, Te-doped GaSb was used to replace some of the nominally undoped GaSb (residual P-type background) starting material. To obtain a high electron concentration, pellets of Sb<sub>2</sub>Te<sub>3</sub> were added to the growth solution. The layers were around 2.0 μm thick. The chemical stoichiometry of the epilayers is roughly In<sub>0.14</sub>Ga<sub>0.86</sub>As<sub>0.13</sub>Sb<sub>0.87</sub>, and was determined by EDS in a scanning electronic microscope. PL measurements were obtained using the 488 nm line of an Ar-ion laser at different exciting powers in the range from 40 to 200 mW. The PL measurements were carried out in a closed-cycle helium cryostat at 15 K. The radiative emission was analysed through an Acton monochromator, and detected with an EG&G Judson InSb infrared detector, cooled with liquid nitrogen. Assignment of each transition was accomplished studying the behaviour of the PL spectra at different excitation powers. The energy positions and the linewidth at half-maximum (FWHM) of each peak have been determined by multi-Gaussians deconvolution of the spectra. In<sub>0.14</sub>Ga<sub>0.86</sub>As<sub>0.13</sub>Sb<sub>0.87</sub> layers with different tellurium concentrations were grown by LPE by adding small quantities of Te to the growth solution as indicated in table 1.

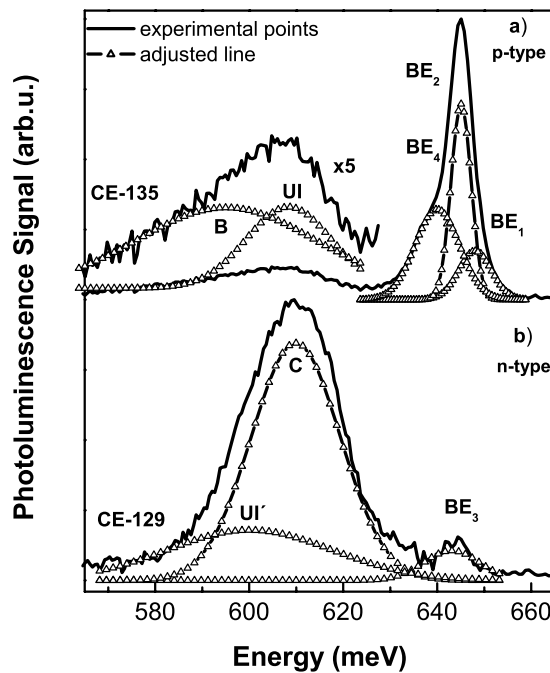


**Figure 1.** (a) Photoluminescence spectra of undoped and (b) slightly N-type InGaAsSb layers measured at 15 K.

### 3. Results and discussion

Figure 1(a) illustrates a 15 K photoluminescence spectrum of an unintentionally doped P-type quaternary alloy, labelled CE-135. This spectrum presents two well-resolved bands as resulted from Gaussians deconvolution. The main band presents three transitions at 648.1, 645.1 and 640.0 meV, which are associated with excitonic transitions labelled by BE. The other band is associated with donor–acceptor transitions named UI and B, respectively [3, 4]. The full width at half maximum (FWHM) of the three PL main bands are 7.0, 4.3 and 9.4 meV, respectively. The FWHM BE bands are smaller than or comparable to the best results previously reported on layers of similar composition grown by LPE and other techniques. These bands do not noticeably change their energetic position when the laser power is increased. We suggest that the transitions labelled as BE are associated with the decay of excitons bound to neutral acceptors. Our assignment is primarily based on the value of its linewidth at half-maximum [4]. Thus, if one assumes that BE<sub>3</sub> is an acceptor-bound exciton transition, an estimation of the band gap is obtained by adding 4 meV (namely, the sum of the exciton dissociation energy and FE binding energy) to the transition energy of BE, namely 648.6 meV. This gives a band gap of 653 meV. In addition to the above discussed transitions, the PL spectrum also presents other transitions corresponding to free electron to acceptor recombination or a donor–acceptor sited at 608.4 meV, named UI. This acceptor has a binding energy of approximately 44 meV. In GaSb and its alloys the donor levels are shallow ( $\sim 2\text{--}3$  meV) due to the small effective mass of the electron, which makes it difficult to distinguish between free-to-bound exciton and excitonic recombination processes. Tellurium has been reported as a shallow N-type impurity for GaSb and its alloys.

For a slightly tellurium-doped InGaAsSb epitaxial layer the low-temperature PL spectrum presents some important differences compared to the undoped layer spectrum (P-type), see

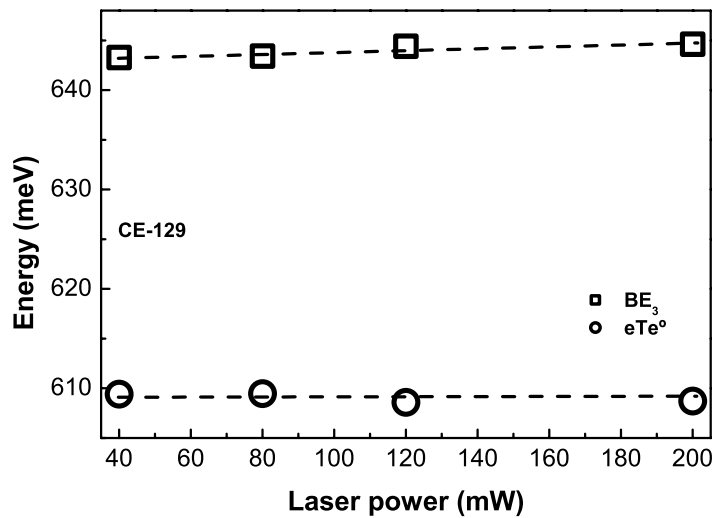


Figure 2. Peak energetic position as a function of laser power to the slightly doped sample, CE-129.

figure 1(b). It shows two main emission bands centred at 643.1 and 609.9 meV, denoted by BE<sub>3</sub> and C, respectively. These bands are associated with band-to-band and tellurium–acceptor transitions (Te<sup>0</sup>A<sup>0</sup>), this last one being the dominant transition. This assignment is not easy, because the energetic position is very close to the radiative transition labelled by UI, although this one is more intense and better resolved. The peak energies did not shift appreciably when the laser power was increased; although it is advisable to remember that the Te has a very small binding energy. This is shown in figure 2. The associated acceptor to these radiative transitions may be the same as that of the UI transition, because its binding energy is very close: 43 meV.

Figure 3 illustrates the PL spectra measured at 15 K of all heavily doped samples studied in this work. As one can observe, the PL spectra have similar features and present the same radiative transitions as in the case of light doping of the samples (all the samples were grown under the same experimental conditions). Therefore, the features observed in spectra may be attributed to tellurium incorporated in the layers. Thus, the increase in tellurium concentration above the degeneracy limit results in the substantial broadening of low-temperature spectra. The individual bands due to the band to band (BB) transitions and band to acceptor transitions (C), as can be seen in figure 3, completely overlap each other at free carrier concentrations (sample CE-122). Additionally, at very high concentrations, the low temperature luminescence band becomes highly asymmetric [8]. Also, peak C becomes dominant as the concentration of Sb<sub>2</sub>Te<sub>3</sub> is increased in the melt solution, which reaffirms the above discussed assignment (that is to say peak C is associated with tellurium and means that the concentration of tellurium increases in alloys).

Figure 4 illustrates the main transitions present in the low temperature PL spectra and their dependence on laser power for the heavily doped sample CE-124. As can be observed, the radiative transitions do not shift appreciably in the investigated power range, indicating that the transitions have the same origin as those in the low doping regime.

Figure 5 illustrates peak energetic positions as a function of the [Sb<sub>2</sub>Te<sub>3</sub>] molar fraction taken from experimental results measured at 15 K; this dependence should allow us to deduce the band gap energy for high tellurium concentrations.

In order to account for the peak position of the photoluminescence band at high tellurium concentrations, it is necessary to include not only the usual band filling effect but also band

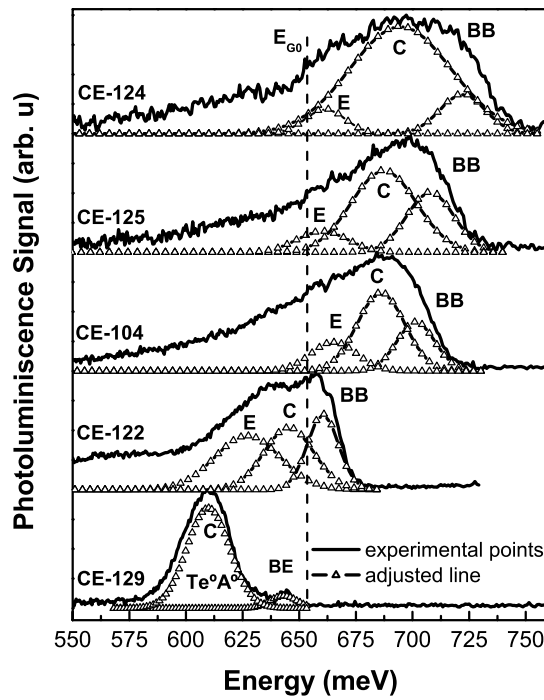


Figure 3. PL spectra of N-type InGaAsSb as a function of  $[\text{Sb}_2\text{Te}_3]$  molar fraction in the growth solution measured at 40 mW excitation power.

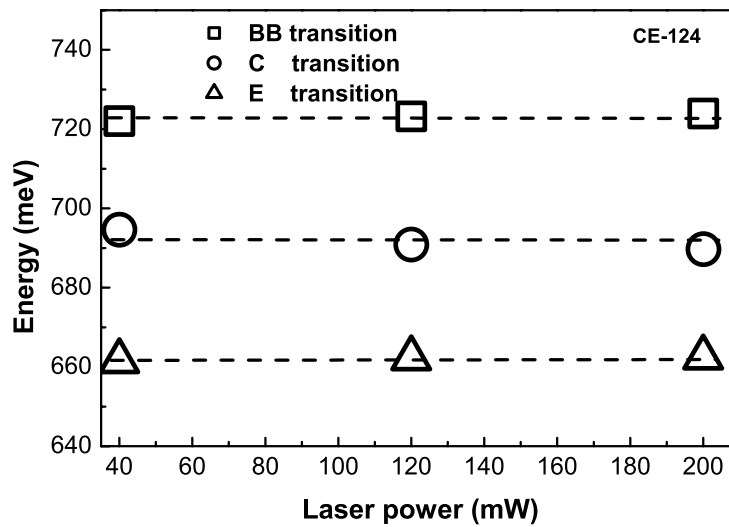
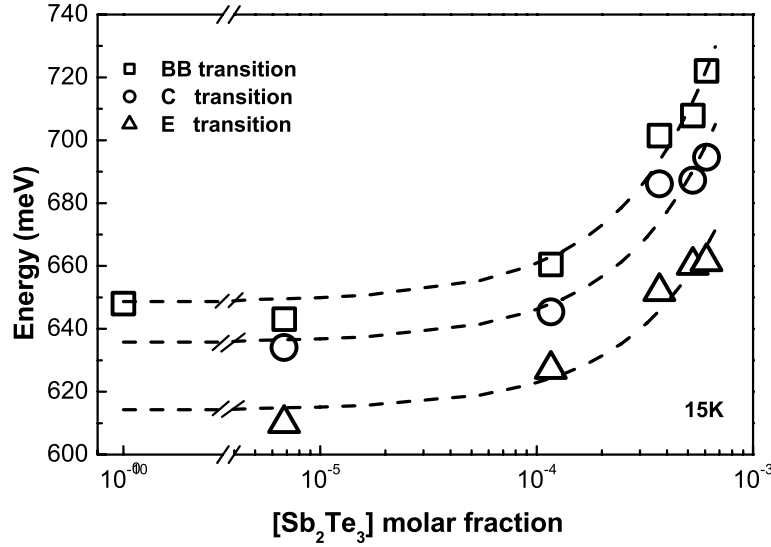


Figure 4. PL Peak energies as a function of the laser power for a heavily doped sample, CE-124.

gap shrinkage due to exchange interaction among free carriers as well as the band tailing effect due to the Coulomb interaction of the free carriers with ionized impurities. All interactions mentioned above are calculated taking into account nonparabolicity of the conduction band, which becomes important for degenerate electron concentrations.



**Figure 5.** Photoluminescence peak position as a function of [Sb<sub>2</sub>Te<sub>3</sub>] molar fraction measured at 15 K. Dashed lines have been fit to the experimental data.

The three-band Kane model [9] has been used for the calculation of the concentration-dependent effective mass of the quaternary alloy. We closely follow the results of [8] for calculating the InGaAsSb concentration-dependent effective mass. Kane showed that the secular determinant has solutions for three of the bands—the conduction band, valence band and spin–orbit split-off band—in the form of a cubic equation

$$E'(E' - E_g)(E' + \Delta) - \hbar^2 k^2 p^2 (E' + (2/3)\Delta) = 0 \quad (1)$$

where  $E' = E - \hbar^2 k^2 / 2m_0^*$ , which is true except at very high energies. A development of the solution of equation (1) in powers of  $k$  up to the order  $k^6$  [10] gives the following expression for the energy of the conduction band as measured from the bottom of the conduction band:

$$E_C = \frac{\hbar^2 k^2}{2m_0^*} + \left(\frac{\alpha}{E_g}\right) \left(\frac{\hbar^2 k^2}{2m_0^*}\right)^2, \quad (2)$$

where  $\alpha$  is defined as

$$\alpha = - \left(1 - \frac{m_0^*}{m_0}\right)^2 \left[ \frac{1 + (\Delta/E_g) + (1/4)(\Delta/E_g)^2}{1 + (4/3)(\Delta/E_g) + (4/9)(\Delta/E_g)^2} \right]. \quad (3)$$

This term is named the nonparabolicity factor. Thus, one can calculate the concentration-dependent effective mass with the following numerical values of In<sub>x</sub>Ga<sub>1-x</sub>As<sub>y</sub>Sb<sub>1-y</sub> band structure parameters:  $m_0^*/m_0 = 0.0354$ ,  $E_g(15 \text{ K}) = 0.653 \text{ eV}$  and  $\Delta = 0.80 \text{ eV}$  [11]. One obtains  $\alpha = -0.733$ . It appears that the nonparabolicity factor is almost independent of temperature. Therefore, we can write the equation for the energy within the conduction band in the following form

$$E_C = E_0 - 0.733(E_0^2/E_g) \quad (4)$$

where  $E_0 = \hbar^2 k^2 / 2m_0^*$ . As the conduction band effective mass is defined by

$$\frac{1}{m^*} = \frac{1}{\hbar^2 k} \left( \frac{\partial E}{\partial k} \right) \quad (5)$$

we can express it in terms of the effective mass at the bottom of the conduction band  $m_0^*$  by the following formula

$$m^* = m_0 [1 - 2 \times 0.733(E_0/E_g)]. \quad (6)$$

For a degenerate semiconductor, a condition which is met in InP at 300 K for electron concentrations exceeding  $\sim 5 \times 10^{17} \text{ cm}^{-3}$ , the wavevector is a function of the free carrier density

$$k = (3\pi^2 n)^{1/3}, \quad (7)$$

which allows us to write the concentration-dependent effective mass for a nonparabolic conduction band of the InGaAsSb alloy in the form

$$m^*(n) = 0.0354m_0(1 - 23.136 \times 10^{-14}n^{2/3})^{-1}. \quad (8)$$

It has been shown that for the variation of  $m^*/m_0$  for InP with electron concentration higher than  $10^{18} \text{ cm}^{-3}$  the assumption of constant effective mass is highly inadequate [8]. This concentration-dependent effective mass expression allows us to obtain a useful expression for the Fermi energy of nonparabolic bands in terms of electron concentration in the following way:

$$E'_F = \frac{\hbar^2 k^2}{2m_d^*} = (3\pi^2)^{2/3} \left( \frac{\hbar^2}{2m_d^*} \right) n^{2/3}. \quad (9)$$

Making use of equations (7) and (8) and by evaluating numerical factors in the equations one can obtain a useful expression for  $E'_F$  in the form

$$E'_F(n) = 10.301 \times 10^{-14}n^{2/3}(1 - 11.563 \times 10^{-14}n^{2/3}) \text{ (eV)} \quad (10)$$

where the free electron concentration is to be substituted in  $\text{cm}^{-3}$ . It has been demonstrated for N-type InP that the Fermi energy calculated by an exact method using Fermi integrals differs only at low concentrations from the Fermi energy of nonparabolic bands obtained above [8]. At high concentrations the values agree very well with calculated values for the case of a nonparabolic band. Now we will analyse each component of the band gap of heavily doped N-type InGaAsSb.

For screened Coulomb potentials the band shift due to the electron–impurity interaction  $E_c^c$  has been calculated by Hwang [12]

$$E_c^c = e^2 (N_D - N_A) / \varepsilon_r \varepsilon_0 Q^2, \quad (11)$$

where  $Q^2$  is the square of the reciprocal screening length defined by

$$Q^2 = (L_s^2)^{-1}. \quad (12)$$

In the case of a degenerate semiconductor the screening length is dependent on the free carrier concentration according to Casey [13]:

$$L_s = (\varepsilon_r \varepsilon_0 \hbar^2 / m^* e^2)^{1/2} (\pi/3)^{1/6} (1/n)^{1/6}. \quad (13)$$

Using the equation for the concentration-dependent effective mass we obtain the following equation for  $E_c^c$  which is valid in the case of InGaAsSb alloys with nonparabolic bands

$$E_c^c(n) = 6.868 \times 10^{-14}n^{2/3}(1 - 23.136 \times 10^{-14}n^{2/3}) \text{ (eV)}. \quad (14)$$

For the derivation it has been assumed that  $N_D - N_A = n$ . Finally, the shrinkage of the band gap due to exchange interaction among free carriers is given according to Camassel [14] by

$$E_c^e(n) = 1.92 \times 10^{-8}n^{1/3} \text{ (eV)} \quad (15)$$



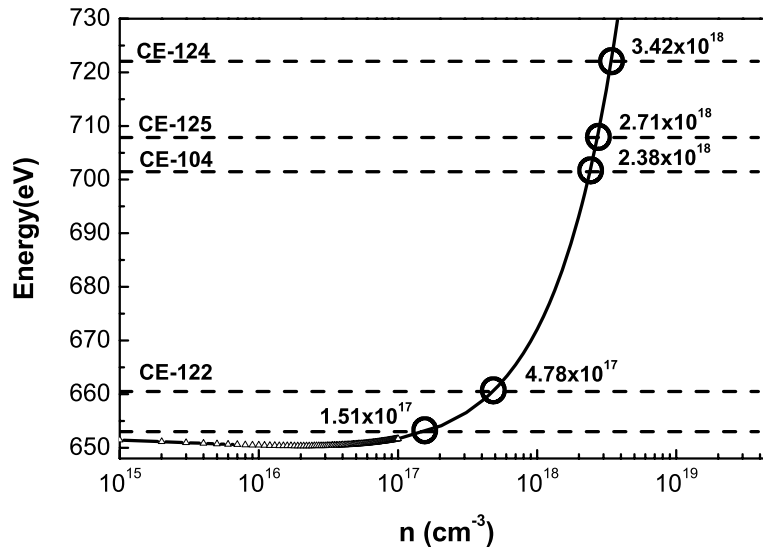


**Figure 6.** Band-to-band transition for N-type InGaAsSb samples as a function of free carrier concentration.

where we have evaluated the numerical factors to simplify the expression. The equation is valid only if the ratio of intercarrier spacing to the Bohr radius in the crystal is  $\leq 1$ .  $E_c^e$  is the energy value by which the band gap of the material is diminished compared with the one-electron band gap.

For the calculation of the peak position of the photoluminescence spectra we assume that the electron distribution is degenerate, whereas the holes introduced by optical generation occupy the states at the very top of the valence band. Therefore, to a good approximation, the peak of the photoluminescence band arising from band-to-band (BB) transition is given by [8]

$$E_p(n) = E_{g0} + E_F'(n) - E_c^e(n) - E_c^e'(n). \quad (16)$$

$E_{g0}$  is the unperturbed band gap of InGaAsSb measured at 15 K. This mathematical expression is a transcendental function which has been used for estimating the electron concentration in the layers. The obtained results are presented in table 1 and are plotted in figure 6. In the concentration range up to  $10^{18} \text{ cm}^{-3}$  a downward shift of the photoluminescence peak is observed due to the predominance of band shrinkage resulting from combined exchange and Coulomb interactions over the band filling. For concentrations exceeding  $10^{18} \text{ cm}^{-3}$  the situation is reversed and a very large shift towards higher energies is observed.

#### 4. Conclusions

In this work we have analysed the low-temperature PL spectra of N-type InGaAsSb epitaxial layers grown by LPE as a function of impurity concentration. The photoluminescence has been studied in the molar fraction range from  $1.16 \times 10^{-4}$  to  $6.09 \times 10^{-4}$ . The low temperature PL spectra for low tellurium concentrations exhibit band-to-band and donor–acceptor transitions, but as the doping increases in the layers the BB transition becomes dominant, indicating that it depends strongly on the tellurium concentration. The band-to-band transition becomes broad and asymmetric, being displaced to high energies. An important result of our analysis is

that nonparabolicity of the conduction band has to be taken into account in calculating the peak position of photoluminescence spectra at degenerate concentrations and in estimating the electron concentration for the grown samples.

### Acknowledgments

The authors want to thank P Rodriguez for her help in growing the epitaxial layers. This work was supported by the CONACYT/Mexico grant 42286-F.

### References

- [1] Shibata S, Horiguchi M, Jingji K, Mitachi S, Kanamori T and Manaba T 1981 *Electron. Lett.* **17** 775
- [2] Chow D H, Miles R H, Hasenberg T C, Kost A R, Zhang Y H, Dunlap H L and West L 1995 *Appl. Phys. Lett.* **67** 3700
- [3] Iyer S, Hedge S, Abul-Fadl A, Bajaj K K and Mitchel W 1993 *Phys. Rev. B* **47** 1329
- [4] Chidley E T R, Haywood S K, Henriques A B, Mason N J, Nicholas R J and Walker P J 1991 *Semicond. Sci. Technol.* **6** 45
- [5] Raccach P M, Rahemi H, Zehnder J, Hawrylo F Z, Kressel H and Helman J S 1981 *Appl. Phys. Lett.* **39** 496
- [6] Hawrylo F Z 1980 *Appl. Phys. Lett.* **37** 1038
- [7] Díaz-Reyes J, Cardona-Bedoya J A, Gómez-Herrera M L, Herrera-Pérez J L, Riech I and Mendoza-Álvarez J G 2003 *J. Phys.: Condens. Matter* **15** 8941
- [8] Bugajski M and Lewandowski W 1985 *J. Appl. Phys.* **57** 521
- [9] Kane E O 1957 *J. Phys. Chem. Solids* **1** 249
- [10] Raymond A, Robert J L and Bernard C 1979 *J. Phys. C: Solid State Phys.* **12** 2289
- [11] Muñoz M, Wei K, Pollak F H, Freeouf J L, Wang C A and Charache G W 2000 *J. Appl. Phys.* **87** 1780
- [12] Hwang C J 1980 *Phys. Rev. B* **2** 4117
- [13] Casey H C Jr and Panish M B 1978 *Heterostructure Laser, Part 1: Fundamental Principles* (New York: Academic) p 135
- [14] Camassel J, Auvergne D and Mathieu H 1975 *J. Appl. Phys.* **46** 2683